Radius anomaly in the diffraction model for heavy-ion elastic scattering

L. N. Pandey and S. N. Mukherjee
Department of Physics, Banaras Hindu University, Varanasi, India
(Received 6 September 1983)

The elastic scattering of heavy ions, ^{20}Ne on ^{208}Pb, ^{20}Ne on ^{235}U, ^{84}Kr on ^{208}Pb, and ^{84}Kr on ^{232}Th, is examined within the framework of Frahn's diffraction model. An analysis of the experiment using the "quarter point recipe" of the expected Fresnel cross sections yields a larger radius for ^{208}Pb than the radii for ^{235}U and ^{232}Th. It is shown that inclusion of the nuclear deformation in the model removes the above anomaly in the radii, and the assumption of smooth cutoff of the angular momentum simultaneously leads to a better fit to elastic scattering data, compared to those obtained by the earlier workers on the assumption of sharp cutoff.

[NUCLEAR REACTIONS Elastic scattering, ^{20}Ne+^{208}Pb (161.2 MeV), ^{20}Ne+^{235}U (175 MeV), ^{84}Kr+^{208}Pb (500 MeV), ^{84}Kr+^{232}Th (500 MeV), diffraction model, nuclear deformation.]

I. INTRODUCTION

The semiclassical aspects of the heavy-ion elastic collisions are well reproduced by Frahn's diffraction model, which has been well reviewed by Frahn and Rehm.[1] The well-known features in the angular distributions of heavy-ion elastic collisions closely resemble the characteristics of Fresnel diffraction in optics. The Fresnel effects are associated with a strong Coulomb field and high projectile energy. The semiclassical Fresnel cross section has the property that its ratio to the Rutherford cross section falls to one quarter at an angle θ_c, corresponding to the critical angular momentum l_c. This is the well-known "quarter point recipe."

The analysis of experimental data using the above-mentioned quarter point recipe of Frahn's diffraction theory leads to an anomaly of the target radius. For example, the analysis of the scattering of ^{84}Kr by ^{232}Th and ^{208}Pb reveals that the radius of ^{208}Pb is greater than the radius of ^{232}Th. The apparent anomaly in the determination of the target radius was first indicated by Brink and Rowley,[2] and was later resolved by Rowley,[3] taking nuclear deformation as an adjustable parameter in Frahn's sharp cutoff diffraction model. However, the fit to the elastic scattering data was very poor though the radius anomaly was resolved. This is quite likely because the assumption of sharp cutoff in the angular momentum space makes the model inadequate in several respects. Frahn[4] recently generalized the diffraction model by considering strong absorption and other quantal aspects of heavy-ion collisions. The most important quantities required are the values of critical angular momentum l_c and the width Δ of the l-space "window" of partial waves that take part in elastic and quasielastic collisions.

It is still very much an open question as to what extent the generalized Fresnel model can resolve the radius anomaly. The purpose of the present investigation is to address this problem and to find out whether there is a simple means of simultaneously obtaining quantitative fits to the available heavy-ion elastic scattering data and resolving the radius anomaly if one exists therein. This is achieved by including gradual transition in l space of the elastic partial wave S matrix and the nuclear deformation in the Fresnel model. In addition to this, we have applied the present model to resolve the radius anomaly, found in the diffraction model analysis of elastic scattering data of ^{20}Ne on ^{208}Pb and ^{20}Ne on ^{235}U. Therefore, the present investigation demonstrates the greater scope of the diffraction model in explaining the elastic collision of heavy deformed nuclei with a minimum number of assumptions about heavy-ion interaction.

II. DIFFRACTION SCATTERING FORMALISM

The diffractive collisions of heavy charged particles are predominantly of the Fresnel type. A direct physical description of the Fresnel type of heavy-ion elastic collisions is provided by Frahn's model, which takes advantage of an elastic scattering S matrix for strongly absorbed particles, which is governed by high energy and a strong Coulomb field.

One starts with the usual partial wave expansion of the elastic scattering amplitude for spin zero particles[5]

$$f(\theta)=\frac{i}{2k}\sum_{l=0}^{\infty}(2l+1)(1-S_l)P_l(\cos\theta)\ , \tag{1a}$$

where

$$S_l=\eta_l e^{2i\delta_l}\ . \tag{1b}$$

The evaluation of $f(\theta)$ is based on an approximation of the partial wave series by an integral over the continuous variable $\lambda=l+\frac{1}{2}$; a replacement of S_l, η_l, and δ_l by a continuously differentiable function,

$$S(\lambda)=\eta(\lambda)e^{2i\delta(\lambda)}\ ; \tag{1c}$$

and the employment of the asymptotic form of $P_\lambda(\cos\theta)$. With these changes, $f(\theta)$ takes the form[1]

$$f(\theta)=f^{(+)}(\theta)+f^{(-)}(\theta)\ , \tag{2a}$$

where

$$f^{(\pm)}(\theta)=-\frac{i}{k}\frac{1}{\sqrt{2\pi\sin\theta}}\int_{1/2}^{\infty}d\lambda\,\lambda^{1/2}\eta(\lambda)e^{i\Phi_\pm(\lambda,\theta)} \tag{2b}$$

and

$$\Phi_\pm(\lambda,\theta)=2\delta(\lambda)\mp(\lambda\theta-\pi/4)\ . \tag{2c}$$

The sharp cutoff model corresponds to $\eta(\lambda)=1$ for $\lambda\le\lambda_c$, and $\eta(\lambda)=0$ for $\lambda>\lambda_c$, where λ_c is the critical angular momentum. The critical angle θ_c is given by

$$\lambda_c=n\cot(\theta_c/2)\ , \tag{3}$$

where n is the Sommerfeld parameter. With these conditions, $f(\theta)$ leads to

$$\frac{\sigma(\theta)}{\sigma_R(\theta)}=\tfrac{1}{2}\{[\tfrac{1}{2}-C(W)]^2+[\tfrac{1}{2}-S(W)]^2\}\ , \tag{4}$$

where $C(W)$ and $S(W)$ are Fresnel's cosine and sine integrals and

$$W=\sqrt{2n/\pi}\sin\tfrac{1}{2}(\theta-\theta_c)/\sin\frac{\theta_c}{2}\ .$$

θ_c is the angle at which Fresnel's cross section falls to one quarter of the Rutherford value (the quarter point recipe).

The sharp cutoff model is incapable of describing quantitative features of the elastic scattering cross section since it neglects reflection of partial waves above the barrier, absorption of partial waves below the barrier, and deviations from Rutherford orbits caused by the real part of the nuclear potential. The most important correction is owing to the gradual transition in angular momentum space (λ) of the elastic partial wave S matrix [Eq. (1c)]. The finite width of this transition region is measured by a parameter Δ that defines the size of the λ-space "window" through which the elastic scattering and most quasielastic reactions proceed. Its effect on the scattering amplitude is described by a function $F(\Delta x)$, defined as the Fourier transform[6] of the derivative $D(\lambda)=d\eta(\lambda)/d\lambda$,

$$F(\Delta x)=\int_{-\infty}^{\infty}d\lambda\,D(\lambda)\exp[i(\lambda-\lambda_c)x]\ . \tag{5}$$

With the following form of reflection function,[4]

$$\eta(\lambda)=\left[1+\exp\left[\frac{\lambda-\lambda_c}{\Delta}\right]\right]^{-1}\ , \tag{6a}$$

we have

$$F[\Delta(\theta_c-\theta)]=\frac{\pi\Delta(\theta_c-\theta)}{\sinh[\pi\Delta(\theta_c-\theta)]}\ . \tag{6b}$$

$F(0)=1$ preserves the quarter point property of the simple Fresnel formula: $\sigma/\sigma_R=\frac{1}{4}$ at $\theta=\theta_c$. The generalized Fresnel formula for the differential cross section, with the assumption of "smooth cutoff," is then given in terms of Fresnel integrals $C\equiv C(\,|\,W\,|\,)$ and $S\equiv S(\,|\,W\,|\,)$ by

$$\frac{\sigma(\theta)}{\sigma_R(\theta)}=1+\tfrac{1}{2}[(\tfrac{1}{2}-C)^2+(\tfrac{1}{2}-S)^2]F^2+(C+S-1)F \quad \text{for } \theta\le\theta_c\ , \tag{7a}$$

$$\frac{\sigma(\theta)}{\sigma_R(\theta)}=\tfrac{1}{2}[(\tfrac{1}{2}-C)^2+(\tfrac{1}{2}-S)^2]F^2 \quad \text{for } \theta\ge\theta_c\ , \tag{7b}$$

where $F\equiv F[\Delta(\theta_c-\theta)]$ is a real function.

III. CALCULATION OF λ_c FROM THE INTERACTION POTENTIAL OF DEFORMED NUCLEI

The diffraction model described in the preceding section assumes that there is a certain critical angular momentum λ_c for which the height of the barrier formed by the Coulomb, centrifugal, and real parts of the nuclear potential is equal to the center of mass energy of the reaction, i.e.,

$$V_C(R)+V_\lambda(R)+V_N(R)=E\ , \tag{8a}$$

where

$$V_C(r)=\frac{Z_TZ_Pe^2}{r},\quad V_\lambda(r)=\frac{\hbar^2\lambda^2}{2\mu r^2}\ ,$$

and μ denotes the reduced mass. The position R of the barrier is determined by

$$\frac{\partial}{\partial r}[V_C(r)+V_\lambda(r)+V_N(r)]_{r=R}=0\ , \tag{8b}$$

where the nuclear potential $V_N(r)$ is obtained by folding the density distribution of the projectile with the real part of the single nucleon optical potential of the target.[13] For spherical nuclei, this potential is approximately given by

$$V_N(r)=V_0\exp\{-[r-(R_P+R_T)]/T\}\ . \tag{9a}$$

For a deformed nucleus, R_P and R_T are given by

$$R_i=R_{0i}(1+\beta_iY_{2,0}) \tag{9b}$$

where $i=P$ or T, β denotes the quadrupole deformation present in the projectile and/or target, and $R_{0i}=r_{0i}A_i^{1/3}$. Substituting the various potentials in Eq. (8b) and differentiating, we get

$$R\simeq D(1+X)\ , \tag{10}$$

where $X=x/D$,

$$x=\sum_{i=P,T}R_{0i}\beta_iY_{2,0}\ ,$$

and D is the position of the barrier when nuclei are not deformed. Finally, we get the following relation between the critical angle θ_c or λ_c and the deformation parameter:

$$\left[\frac{\lambda_c}{n}\right]^2=\cot^2(\theta_c/2)$$
$$\simeq\cot^2(\theta_c^0/2)(1+X)^2+4\alpha X(1+X)\ , \tag{11}$$

where θ_c^0 is the critical angle for $X=0$, $\alpha=E/V_C^0$, and V_C^0 is the Coulomb potential at $r=D$ or $X=0$.

TABLE I. Parameters used to calculate nucleus-nucleus interactions. i=projectile or target.

Nuclei	ρ_0 (fm^{-3})	V_0 (MeV)	Surface thickness (fm)	R_{0i} (fm)
Projectile	0.186		0.54	$1.04A_P^{1/3}$
Target		−50.0	0.65	$r_{0T}A_T^{1/3}$

IV. FOLDING MODEL POTENTIAL

The long range part of the nucleus-nucleus interaction is obtained by folding the density distribution of the projectile nucleus with the real part of the single nucleon optical potential of the target nucleus as follows[7,13]:

$$V_N(r)=\int \rho_P(r_P)V_T(r_P-r)d^3r_P\ , \tag{12}$$

where $\rho_P(r_P)$ is the density of the projectile nucleus, and V_T ($r_T=r_P-r$) is the real part of the single nucleon optical potential for the target nucleus. When ρ_P and V_T both have spherical symmetry, the integral of Eq. (12) becomes a two-dimensional integral:

$$V_N(r)=\frac{\pi}{4r}\int_\gamma^\infty ds\int_{-\nu}^{\nu}dt\,\rho_P\left[\frac{s+t}{2}\right]V_T\left[\frac{s-t}{2}\right](s^2-t^2)\ , \tag{13}$$

where $s=r_T+r_P$ and $t=r_P-r_T$.

When ρ_P and V_T have the Woods-Saxon form with the same surface thickness, the integral of Eq. (13) can be evaluated analytically,

$$V_N(r)=\frac{\pi\rho_0V_0}{4r}f(r)\ , \tag{14a}$$

and

$$V_N'(r)=-\frac{\pi\rho_0V_0}{4r}[f(r)/r+I(r)]\ , \tag{14b}$$

where

$$I(r)=\frac{g(r)}{\exp\left[\dfrac{r-R_0}{T}\right]-1}\ , \tag{14c}$$

TABLE II. Quadrupole deformation parameters β used in the calculation.

Nuclei	^{20}Ne	^{84}Kr	^{208}Pb	^{235}U	^{232}Th	^{209}Bi
β	0.870	0.207	0.000	0.259	0.267	0.000

$$f(r)=-Tg(r+T)\ln\left[1-\exp\left[\frac{R_0-r}{T}\right]\right]\ , \tag{14d}$$

$$g(r)=(r-R_0)\left[2r^2-\frac{8\pi^2T^2}{3}\right]-\tfrac{1}{3}[(r-2R_P)^3+(r-2R_T)^3]\ , \tag{14e}$$

and

$$R_0=R_p+R_T\ .$$

Here, V_0 denotes the depth of the Woods-Saxon well and ρ_0 is chosen such that the normalization of ρ_P gives the mass number of the projectile.

V. NUMERICAL CALCULATIONS

Now we will describe the numerical determination of the quarter point for collisions of ^{20}Ne on ^{208}Pb at 161.2 MeV, ^{20}Ne on ^{235}U at 175 MeV, ^{84}Kr on ^{208}Pb at 500 MeV, and ^{84}Kr on ^{232}Th at 500 MeV. Our aim is to compare the calculated quarter points with those obtained directly from experimental data.

First, we solve Eq. (8b) to find the position of the barrier, D, by changing the separation distance between target and projectile in steps of 0.001 fm and keeping their radii fixed. $V_N(r)$ and $V_N'(r)$ are calculated from Eq. (14), taking both nuclei spherical ($\beta_i=0$) and of equivalent surface thickness

$$T=2\prod_i T_i\Big/\sum_i T_i\ .$$

The parameters used for calculating nucleus-nucleus interactions are taken from the work of Brogila and Winther[7] and are given in Table I. The value $[V_N(r)]_{r=D}$ is then calculated by numerical integration (24 points Gaussian quadrature) of Eq. (13). Substituting $V_N(D)$, $V_C^0(D)$, and E in Eq. (8a), we get the critical angular momentum

TABLE III. The target radius calculated on the basis of the quarter point recipe with and without nuclear deformation.

Nuclear reactions		Radius of target nucleus: Without deformation			With deformation			Experimental quarter point properties	
Projectile	Target	r_{0T} (fm)	R_{0T} (fm)	θ_c^0	r_{0T} (fm)	R_{0T} (fm)	θ_c^0	θ_c	λ_c
^{20}Ne	^{235}U	1.238	7.64	56.2	1.439	8.88	52.86	56.2	92.1
^{20}Ne	^{208}Pb	1.300	7.70	53.1	1.430	8.47	51.03	53.1	91.0
^{84}Kr	^{232}Th	1.109	6.81	125.0	1.232	7.57	116.30	125.01	108.4
^{84}Kr	^{208}Pb	1.181	7.00	101.0	1.228	7.28	98.94	101.0	156.6

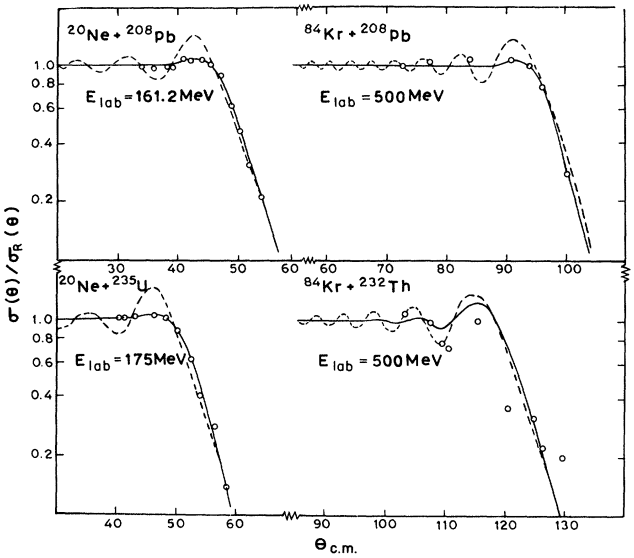

FIG. 1. The elastic scattering cross section $\sigma(\theta)/\sigma_R(\theta)$ of heavy ions with sharp cutoff (dotted line) and smooth cutoff (solid line). The circles represent the experimental values, taken from Refs. 8–11.

λ_c^0 and hence the critical angle θ_c^0. This process is repeated by varying r_{0T} in steps of 0.0001 fm until the calculated critical angle agrees with the experimental value. The determination of the quarter point within the framework of the diffraction model discussed above leads consistently to an anomaly in the radius of the target in question. For example, the radius of a low mass nucleus turns out to be greater than that of a high mass nucleus. Furthermore, we also find that the radius of the same target changes with the incident energies.

The above apparent anomaly can be resolved by considering nuclear deformation described by Eq. (9b). The values of β_i used in the calculations are taken from Ref. 12 and are given in Table II. The above procedure is then again repeated to find λ_c and θ_c.

VI. RESULTS AND DISCUSSION

Having found the target radius from the quarter point analysis with and without nuclear deformation, it is of some interest to compare the resultant radius and the elastic cross section. We see from Table III that the inclusion of the nuclear deformation will yield a consistently greater radius for heavy mass nuclei compared to light mass nuclei. For example, the radii of ^{235}U and ^{232}Th are found greater than that of ^{208}Pb, as expected. However, this is not the case when the deformation is excluded. Our present analysis differs from that of Rowley[3] in the sense that the latter used nuclear deformation as a variational parameter. The kinetic energy of relative motion in the region of the barrier is large compared with the energies of rotational levels of these nuclei, and they might not have time to change their shape and size appreciably. Therefore, it is physically more meaningful to use intrinsic deformation of nuclei determined from the experimental value of the ground state quadrupole moment as shown in Table II.

Table III also shows the values of θ_c^0 which one would obtain for scattering of spherical nuclei of radii R_{0P} and R_{0T}. It is interesting to note that the nuclear deformation has pushed out the actual quarter point θ_c^0 to θ_c, and hence explains the cause of the radius anomaly.

Furthermore, we are able to achieve a much better fit to the elastic scattering cross-section data, as shown in Fig. 1, with the help of the smooth cutoff model (solid line) instead of the sharp cutoff model (dotted line) used by previous workers.[2,3,11,16] The parameters Δ used in the smooth cutoff model are 6.5 for ^{20}Ne on ^{235}U, 5.0 for ^{20}Ne on ^{208}Pb, 2.7 for ^{84}Kr on ^{232}Th, and 6.2 for ^{84}Kr on ^{208}Pb. The smooth cutoff model, aside from the "cosmetic" effect of giving much better fits of the data, provides additional information through the parameter Δ. We also notice that there are large variations in the diffuseness parameter[4]

$$d = \Delta / K\sqrt{1+(n/\lambda_c)^2} ,$$

where K is the wave number. Particularly, its values for heavier projectiles are substantially smaller than for the lighter projectiles. This is most likely to be attributed to the quasielastic contamination of very heavy-ion data.

In order to test the consistency of the quarter point analysis, the calculation is carried for the same target-projectile system at different incident energies. The quarter point properties are shown in Table IV and the corresponding fits to the elastic scattering data are shown in Fig. 2.

TABLE IV. Results for ^{20}Ne on ^{235}U and ^{84}Kr on ^{209}Bi at different energies.

Nuclear reactions			Radius of target		Experimental quarter point properties	
Projectile	Target	E_{lab} (MeV)	r_{0T} (fm)	R_{0T} (fm)	θ_c	λ_c
^{20}Ne	^{235}U	175	1.238	7.64	56.2	92.1
^{20}Ne	^{235}U	252	1.280	7.90	33.8	134.8
^{84}Kr	^{209}Bi	600	1.305	7.75	66.7	270.0
^{84}Kr	^{209}Bi	712	1.334	7.92	50.5	343.0
^{84}Kr	^{209}Bi	714	1.356	8.05	49.5	350.0

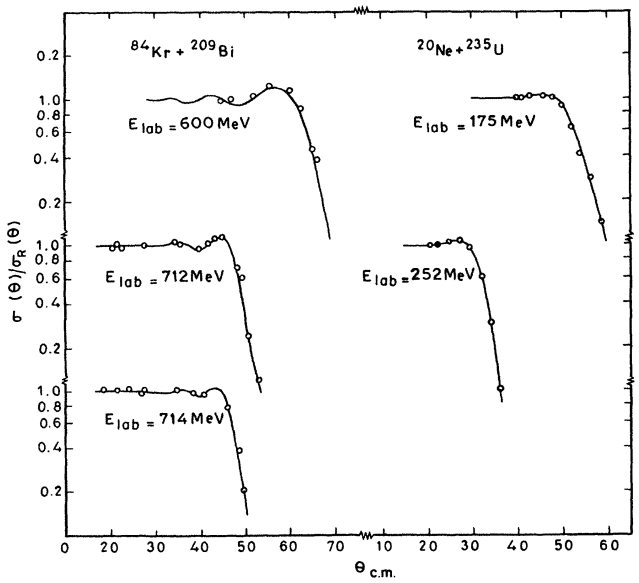

FIG. 2. The elastic scattering cross section $\sigma(\theta)/\sigma_R(\theta)$ of ^{20}Ne on ^{235}U and ^{84}Kr on ^{209}Bi at different incident energies. The circles represent the experimental values taken from Refs. 8 and 11.

Recently, through a similar analysis, Pandey[14] found that the target radius anomaly is not only confined to very heavy deformed nuclei, but the same could be seen in the elastic collision data[15] of light deformed nuclei.

VII. CONCLUSIONS

We make the following essential conclusions from the present investigation:

The addition of nuclear deformation in the Fresnel diffraction model resolves the radius anomaly, and the assumption of smooth cutoff of the angular momentum leads to a better fit to the elastic heavy-ion collision data. The presence of the angular momentum space window width, aside from its cosmetic effects, provides additional information about the nonelastic events. Clearly, by analyzing a substantial amount of data one can hope to give a valid description of collisions of heavy-ion deformed nuclei in terms of semiclassical diffraction models on par with the optical model analysis.

ACKNOWLEDGMENTS

We are grateful to Professor W. E. Frahn for providing us with much useful information regarding the present investigation. We also thank the members of the Nuclear Reaction group at the Variable Energy Cyclotron Centre, Bhabha Atomic Reserach Centre, Calcutta, for their kind hospitality. Finally, the financial assistance provided by the Department of Atomic Energy, Government of India, is gratefully acknowledged.

[1]W. E. Frahn and K. E. Rehm, Phys. Rep. 37C, 1 (1978); W. E. Frahn and D. H. E. Gross, Ann. Phys. (N.Y.) 101, 520 (1976).
[2]D. M. Brink and N. Rowley, Nucl. Phys. A219, 79 (1974).
[3]N. Rowley, Nucl. Phys. A219, 93 (1974).
[4]W. E. Frahn, Nucl. Phys. A302, 267 (1978); A302, 281 (1978).
[5]W. E. Frahn, Ann. Phys. (N.Y.) 72, 524 (1972).
[6]J. A. McIntyre, K. H. Wang, and L. C. Becker, Phys. Rev. 117, 1337 (1960); W. E. Frahn and R. H. Venter, Ann. Phys. (N.Y.) 24, 243 (1963); R. H. Venter, *ibid.* 25, 405 (1963).
[7]R. A. Brogila and A. Winther, Phys. Rep. 4C, 153 (1972).
[8]W. G. Meyer, R. G. Clark, V. E. Viola, Jr., R. G. Sextro, and A. M. Zebelman, Z. Phys. A 277, 141 (1976).
[9]J. B. Ball, C. B. Fulmer, E. E. Gross, M. L. Halbert, D. C. Hernley, C. A. Rudemann, M. J. Saltmarsh, and G. R. Satchler, Nucl. Phys. A252, 208 (1975).
[10]P. Colombani, J. C. Jacmart, N. Poffe, M. Riou, C. Stephan, and J. Tys, Phys. Lett. 42B, 197 (1972).
[11]J. R. Huizenga, in Proceedings of the Symposium on Macroscopic Features of Heavy Ion Collisions, Argonne National Laboratory, Argonne National Laboratory Report ANL/PHY-76-2, 1976, p. 1.
[12]P. H. Stelson and L. Grodzins, Nucl. Data Tables 1A, 21 (1966); K. E. G. Lobner, M. Vetter, and V. Honing, Nucl. Data Tables A7, 495 (1970); Peter Moller and J. Rayford Nix, At. Data Nucl. Data Tables 26, 165 (1981).
[13]H. Feshbach, Annu. Rev. Nucl. Sci. 8, 49 (1958); G. W. Greenlees, G. J. Pyle, and Y. C. Tang, Phys. Rev. 171, 1115 (1968); H. Kidwai and J. R. Rock, Nucl. Phys. A169, 417 (1971).
[14]L. N. Pandey, Ph.D. thesis, Banaras Hindu University, 1983 (unpublished).
[15]J. Nurzynski, C. H. Atwood, T. R. Ophel, D. F. Hebbard, B. A. Robson, and R. Smith, Nucl. Phys. A399, 259 (1983).
[16]J. R. Birkelund, J. R. Huizenga, H. Freiesleben, K. L. Wolf, J. P. Unik, and V. E. Viola, Jr., Phys. Rev. C 13, 133 (1976); J. R. Birkelund, W. U. Schroder, J. R. Huizenga, K. L. Wolf, J. P. Unik, and V. E. Viola, Jr., see Ref. 11, p. 451.